Обзор ArXiv/astro-ph, 3-7 августа 2020

От Сильченко О.К.

ArXiv: 2008.01161

Hot gaseous atmospheres of rotating galaxies observed with *XMM-Newton*

A. Juráňová[1,2,3]★, N. Werner[1,4,5], P. E. J. Nulsen[6,7], M. Gaspari[8,9]†, K. Lakhchaura[10], R. E. A. Canning[11,12], M. Donahue[13], F. Hroch[1], G. M. Voit[13]

[1] *Department of Theoretical Physics and Astrophysics, Masaryk University, Kotlářská 2, 611 37 Brno, Czech Republic*
[2] *SRON Netherlands Institute for Space Research, Sorbonnelaan 2, 3584 CA Utrecht, The Netherlands*
[3] *Anton Pannekoek Institute, University of Amsterdam, Postbus 94249, 1090 GE Amsterdam, The Netherlands*
[4] *School of Science, Hiroshima University, 1-3-1 Kagamiyama, Higashi-Hiroshima 739-8526, Japan*
[5] *MTA-Eötvös Loránd University Lendület Hot Universe Research Group, H-1117 Pázmány Péter sétány 1/A, Budapest, Hungary*
[6] *Harvard-Smithsonian Center for Astrophysics, 60 Garden Street, Cambridge, MA 02138, USA*
[7] *ICRAR, University of Western Australia, 35 Stirling Hwy, Crawley, WA 6009, Australia*
[8] *Department of Astrophysical Sciences, Princeton University, 4 Ivy Lane, Princeton, NJ 08544-1001, USA*
[9] *INAF - Osservatorio di Astrofisica e Scienza dello Spazio, via P. Gobetti 93/3, I-40129 Bologna, Italy*
[10] *MTA-ELTE Astrophysics Research Group, H-1117 Pázmány Péter sétány 1/A, Budapest, Hungary*
[11] *Kavli Institute for Particle Astrophysics and Cosmology, Stanford University, 452 Lomita Mall, Stanford, CA 94305-4085, USA*
[12] *Department of Physics, Stanford University, 382 Via Pueblo Mall, Stanford, CA 94305-4060, USA*
[13] *Physics & Astronomy Department, Michigan State University, East Lansing, MI 48824-2320, USA*

Выборка: картинки

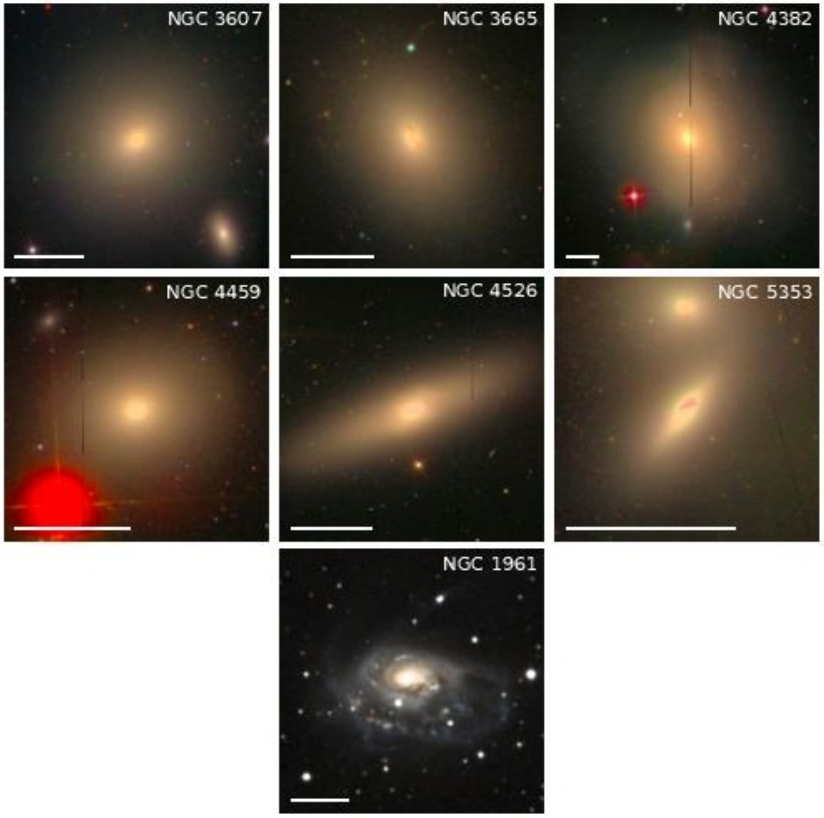

Figure 1. Optical images of the studied sample of S0 galaxies and NGC 1961. The images are taken from Sloan Digital Sky Survey (SDSS, data release 7) with the exception of NGC 1961, which is from Digitized Sky Survey 2. The SDSS images are compositions of g, r, and i (Smith et al. 2002) imaging data. The solid line in the lower-left corner of every image represents a scale of 10 kpc.

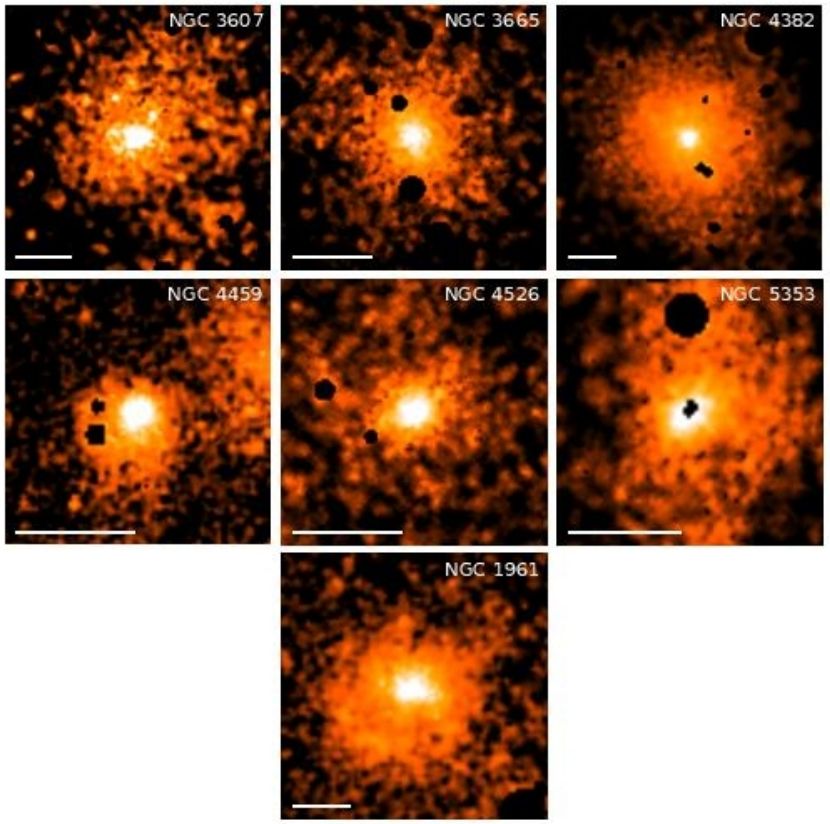

Figure 2. Images of X-ray atmospheres of S0 galaxies in our sample and NGC 1961, all extracted in the energy range 0.3 – 2.0 keV. The images are displayed on log-scale in order to visualize the full extent of the hot atmospheres, while the most prominent point sources have been removed. The solid line in the lower-left corner of every image represents a scale of 10 kpc.

Выборка и результаты в рентгене

object NGC	L_B $10^{10}\,L_{B,\odot}$	$B-V$ mag	$\log P_{\rm radio}$ W Hz^{-1}	$L_{\rm PAH}$ 10^{41} erg s^{-1}	$\log M_{\rm H_2}$ $M_\odot$	$\log M_{\rm H\,I}$ $M_\odot$	SFR $M_\odot\,{\rm yr}^{-1}$
3607	3.70	0.93	20.63	7.8 ± 6.2	8.42	< 6.53	0.420
3665	3.37	0.93	22.04	45.1 ± 9.9	8.91	< 7.05	0.109
4382	5.86	0.89	< 19.79	0.3 ± 5.5	< 7.39	< 6.59	0.002
4459	1.45	0.97	< 19.63	7.1 ± 2.9	8.24	< 6.53	0.071
4526	2.42	0.98	20.61	17.1 ± 4.4	8.59	7.15	0.028
5353	3.56	1.03	21.62	2.3 ± 6.7	< 7.44	< 7.07	0.095
1961	22.91	0.86	22.82	37.8 ± 3.1	10.39	10.67	9.24

NGC	$\varepsilon_{\rm X}$	$\varepsilon_\star$	PA$_{\rm X}$ [deg]	PA$_\star$ [deg]	β	r_0 [pc]
3607	0.144 ± 0.011	0.13 ± 0.08	119.7 ± 2.3	124.8 ± 7.6	0.440 ± 0.007	35 ± 2
3665	0.175 ± 0.005	0.22 ± 0.01	29.0 ± 1.0	30.9 ± 2.0	0.643 ± 0.008	142 ± 3
4382	0.110 ± 0.006	0.25 ± 0.07	29.8 ± 1.7	12.3 ± 11.0	0.349 ± 0.004	31 ± 2
4459	0.060 ± 0.016	0.21 ± 0.03	134.1 ± 7.8	105.3 ± 1.9	0.79 ± 0.06	58 ± 4
4526	0.218 ± 0.005	0.76 ± 0.05	116.8 ± 0.7	113.7 ± 1.2	1.00 ± 0.02	129 ± 3
5353	0.253 ± 0.004	0.48 ± 0.04	136.6 ± 0.6	140.4 ± 4.9	0.86 ± 0.01	157 ± 3
1961	0.161 ± 0.009	0.330	100.8 ± 1.8	92.0 ± 2.0	0.46 ± 0.01	63 ± 3

object NGC	$L_{\rm X}$ 10^{40} erg s^{-1}	$k_{\rm B}T_{\rm X}$ keV	$\sigma_{T_{\rm X}}$ keV	$M_{\rm X}$ 10^9 $M_\odot$	$R_{\rm max}$ kpc
3607	1.74	$0.411^{+0.025}_{-0.009}$	–	$1.52^{+0.07}_{-0.17}$	21.8
3665	2.30	$0.312^{+0.006}_{-0.006}$	–	$1.09^{+0.07}_{-0.07}$	19.1
4382	7.97	$0.316^{+0.025}_{-0.024}$	$0.012^{+0.017}_{-0.012}$	$5.26^{+0.10}_{-0.10}$	36.1
4459	0.31	$0.390^{+0.041}_{-0.014}$	–	$0.12^{+0.02}_{-0.02}$	9.3
4526	0.71	$0.260^{+0.013}_{-0.019}$	–	$0.15^{+0.03}_{-0.02}$	8.5
5353	4.21	$0.651^{+0.020}_{-0.020}$	$0.225^{+0.042}_{-0.046}$	$0.49^{+0.03}_{-0.03}$	11.7
1961	4.79	$0.298^{+0.030}_{-0.082}$	$0.202^{+0.082}_{-0.053}$	$6.01^{+0.49}_{-0.46}$	25.8

To determine the flattening of the atmospheres, we used the CIAO (version 4.12, Fruscione et al. 2006) fitting tool Sherpa (Refsdal et al. 2009) to fit each galaxy with a 2D β-model (Cavaliere & Fusco-Femiano 1976, 1978) of the form

$$I(r) = I_{\rm c}\left[1 + r^2\right]^{-3\beta/2}, \qquad (1)$$

where

$$r^2 = \frac{(1-\varepsilon_{\rm X})^2\tilde{x}^2 + \tilde{y}^2}{r_0^2(1-\varepsilon_{\rm X})^2} \qquad (2)$$

Температура ниже, чем у эллиптических той же массы

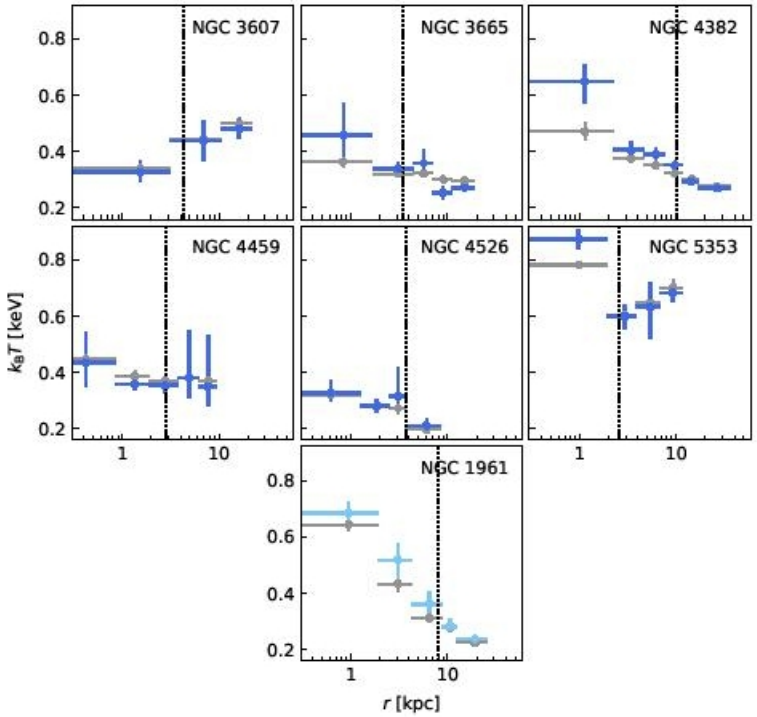

Figure 3. Radial, azimuthally averaged temperature profiles derived from projected (grey) and deprojected (blue) spectra with metallicity fixed at 0.5 $Z_\odot$. For clarity, dark blue points represent S0 galaxies in our sample, while the profile of the spiral galaxy NGC 1961 is plotted in light blue. The effective radius (see Table 1) is represented by the black dotted line in each panel.

А энтропия выше…

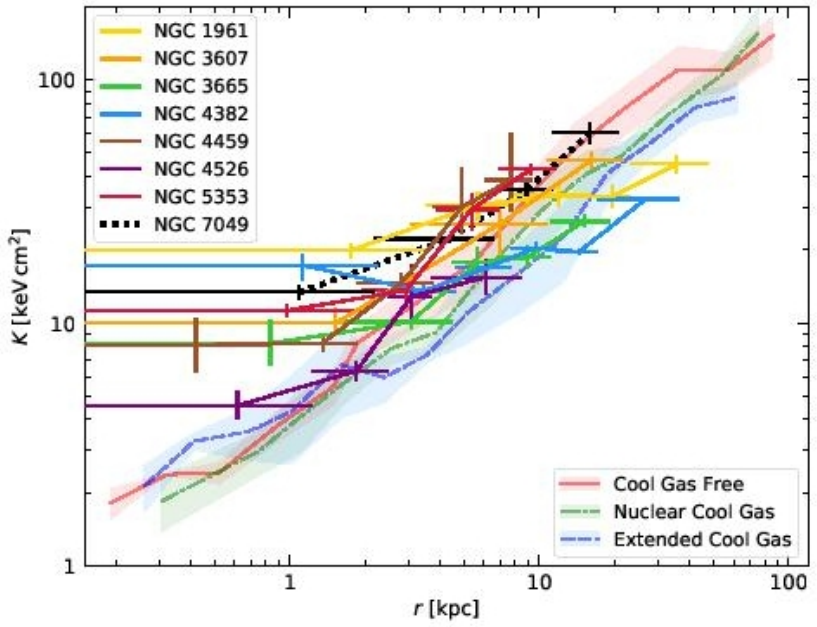

Figure 5. Entropy profiles of the rotationally supported galaxies in this study (solid lines), NGC 7049, an S0 from previous work (Juráňová et al. 2019, black dotted line) and a sample elliptical galaxies distinguished by the extent of cool gas of Lakhchaura et al. (2018). For the ellipticals, lines signify median profiles and surrounding shaded regions the median absolute deviations.

3.2.2 Entropy

A key physical quantity describing the thermodynamic states of hot galactic atmospheres is entropy. We adopt here its definition customary in this field and refer to the entropy index K defined below as the entropy hereafter,

$$K \equiv k_{\rm B} T n_{\rm e}^{-2/3}. \quad (4)$$

This definition relates to the thermodynamic entropy per particle, s, of non-interacting monoatomic particles as $\Delta s = 3/2 k_{\rm B} \ln K$. A gravitationally stratified atmosphere in hydrostatic equilibrium should have an entropy profile rising monotonically with radius, while a flat or decreasing trend would indicate a convectively unstable environment.

Чистая гравитация?

profile given by $K \propto r^{1.1}$, which is usually not observed due to the heating by the AGN and supernovae that centrally increase the gas entropy, flattening the profiles to $K \propto r^{0.67}$ (Panagoulia et al. 2014; Babyk et al. 2018). To

Может ли горячий газ оседать в холодный диск?

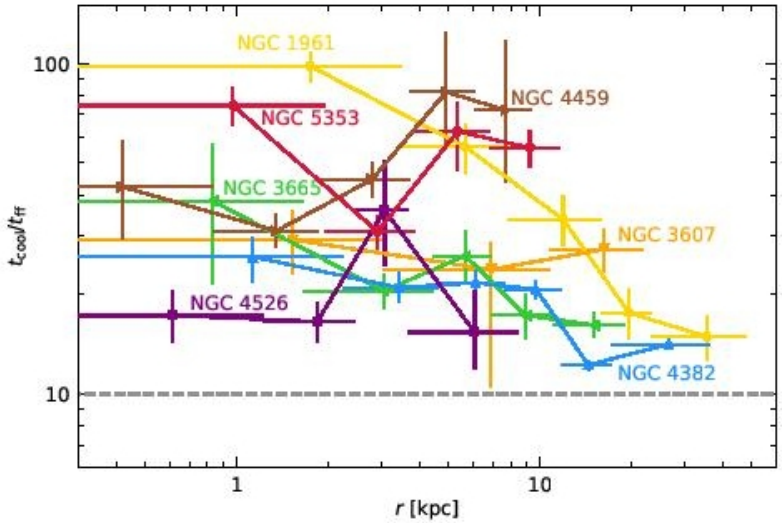

Figure 7. Ratio of cooling time to free-fall time for all studied galaxies. The value $t_{cool}/t_{ff} \approx 10$ (see section 3.3) is visualised as a dashed grey line.

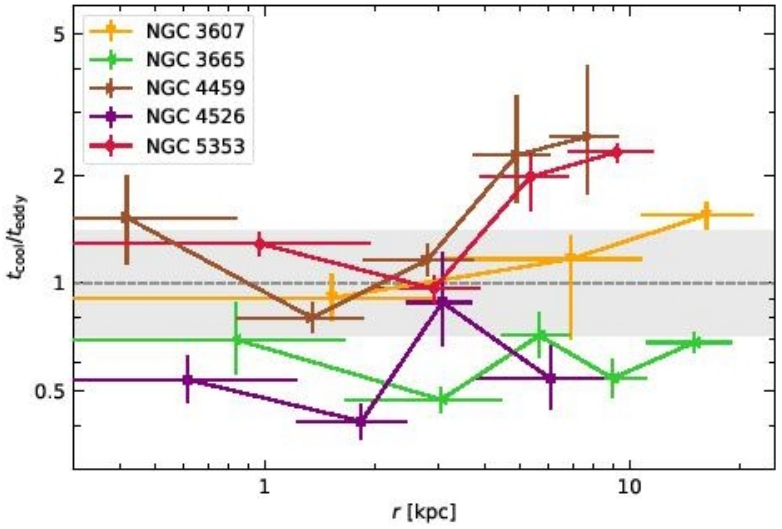

Figure 8. The C-ratio (see section 3.3) of S0 galaxies possessing cold gas. The grey region represents the 1σ confidence region (from hydrodynamical simulations; Gaspari et al. 2018) where conditions for the development of multiphase condensations are expected to be favourable.

Да, если турбулентность рождает многотемпературность...

ArXiv: 2008.02426

The SAMI Galaxy Survey: A Range in S0 Properties Indicating Multiple Formation Pathways

Simon Deeley[1⋆], Michael J. Drinkwater[1], Sarah M. Sweet[1,2,3], Jonathan Diaz[4], Kenji Bekki[4], Warrick J. Couch[2], Duncan A. Forbes[2], Joss Bland-Hawthorn[5], Julia J. Bryant[3,5,6], Scott Croom[3,5], Luca Cortese[3,4], Jon S. Lawrence[7], Nuria Lorente[8], Anne M. Medling[9,10†], Matt Owers[11,12], Samuel N. Richards[13] and Jesse van de Sande[3,5]

[1] *School of Mathematics and Physics, University of Queensland, Brisbane, Queensland 4072, Australia*
[2] *Centre for Astrophysics & Supercomputing, Swinburne University, Hawthorn, VIC 3122, Australia*
[3] *ARC Centre of Excellence for All Sky Astrophysics in 3 Dimensions (ASTRO 3D)*
[4] *International Centre for Radio Astronomy Research, The University of Western Australia, 35 Stirling Highway, Crawley, Western Australia, 600*
[5] *Sydney Institute for Astronomy, School of Physics, The University of Sydney, NSW 2006, Australia*
[6] *Australian Astronomical Optics, AAO-USydney, School of Physics, University of Sydney, NSW 2006, Australia*
[7] *Australian Astronomical Optics - Macquarie, Macquarie University, NSW 2109, Australia*
[8] *AAO-MQ, Faculty of Science & Engineering, Macquarie University. 105 Delhi Rd, North Ryde, NSW 2113, Australia*
[9] *Research School of Astronomy and Astrophysics, Australian National University, Canberra, ACT 2611, Australia*
[10] *Ritter Astrophysical Research Center University of Toledo Toledo, OH 43606, USA*
[11] *Department of Physics and Astronomy, Macquarie University, NSW 2109, Australia*
[12] *Astronomy, Astrophysics and Astrophotonics Research Centre, Macquarie University, Sydney, NSW 2109, Australia*
[13] *SOFIA Science Center, USRA, NASA Ames Research Center, Building N232, M/S 232-12, P.O. Box 1, Moffett Field, CA 94035-0001, USA*

Обзор SAMI

2.1 The SAMI survey

The observational data products used in this work were created by the SAMI Galaxy Survey (Bryant et al. 2015). The Sydney-AAO Multi-object Integral field spectrograph (SAMI; Croom et al. 2012) is mounted at the prime focus of the 3.9m the Anglo-Australian Telescope, which provides a 1 degree diameter field of view. SAMI uses 13 fused fibre bundles (Hexabundles; Bland-Hawthorn et al. 2011; Bryant et al. 2014) with a high (75 percent) fill factor. Each bundle contains 61 fibres of 1.6 arcsec diameter resulting in each hexabundle having a diameter of 15 arcsec. The hexabundles, as well as 26 sky fibres, are plugged into predrilled plates using magnetic connectors. SAMI fibres are fed to the double-beam AAOmega spectrograph (Sharp et al. 2006). For the SAMI Galaxy Survey its 570V grating was used with the blue arm (3700-5700A), giving a resolution of R=1730 (σ = 74km/s), and the R1000 grating with the red arm (6250-7350A) giving a resolution of R=4500 (σ = 29km/s) (van de Sande et al. 2017). At least six pointings on each galaxy are weighted and combined to produce data cubes with a pixel scale of 0.5×0.5 arcseconds (Allen et al. 2015; Sharp et al. 2015). Here we use data products released in Data Release 2 (Scott et al. 2018).

Всего 219 S0, до 1.5 эфф. радиуса: 85 в скоплениях и 134 из GAMA

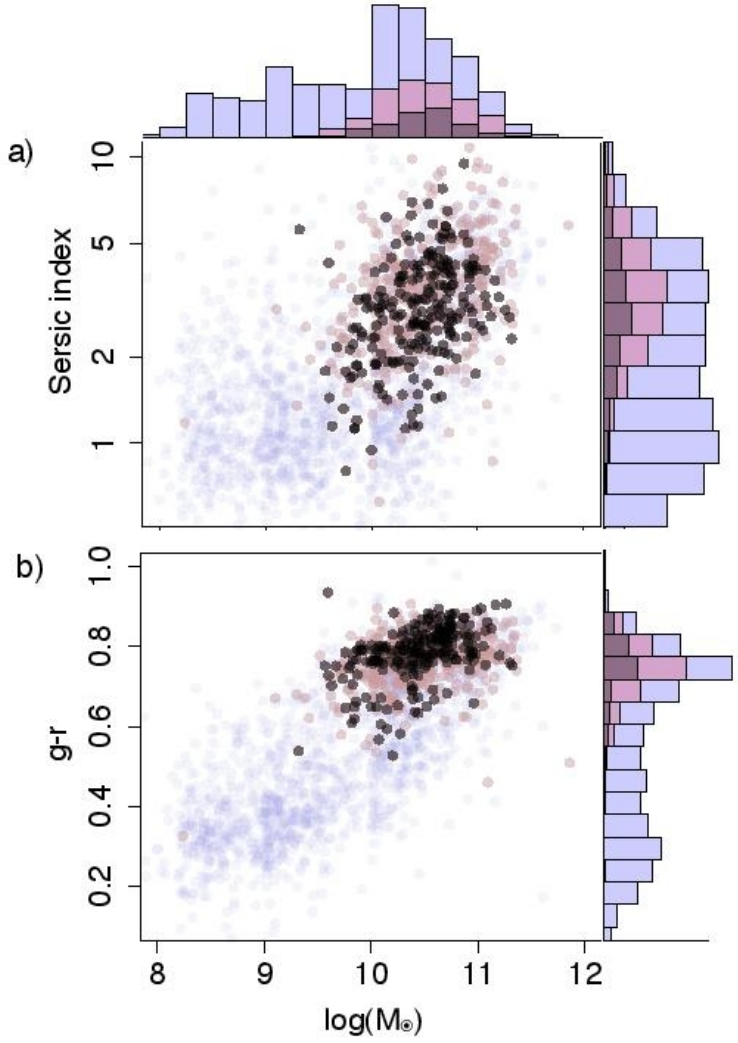

Статистика по поддержке вращением звездных дисков

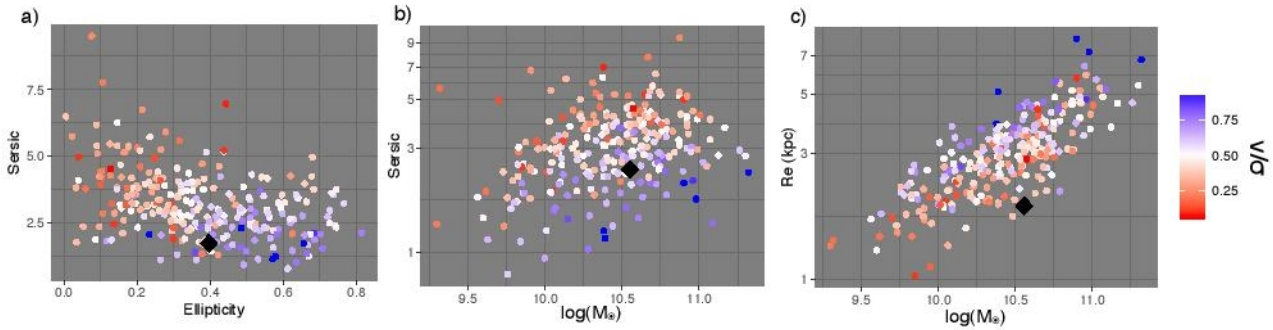

Figure 3. Distributions of our final S0 sample over Sérsic index vs ellipticity (a), vs stellar mass (b) and the effective radii mass (c). Points are shaded according to their v/σ value, with bluer points showing more rotationally-supported S0s. A gradie is evident over each of these parameter spaces, showing that higher rotational support corresponds to lower Sérsic indexes a effective radii. The black diamond corresponds to the locations of the Diaz et al. (2018) fiducial model, which has a stellar $v/$ around 0.2.

Черный ромб - любимая модель Diaz+(2018)

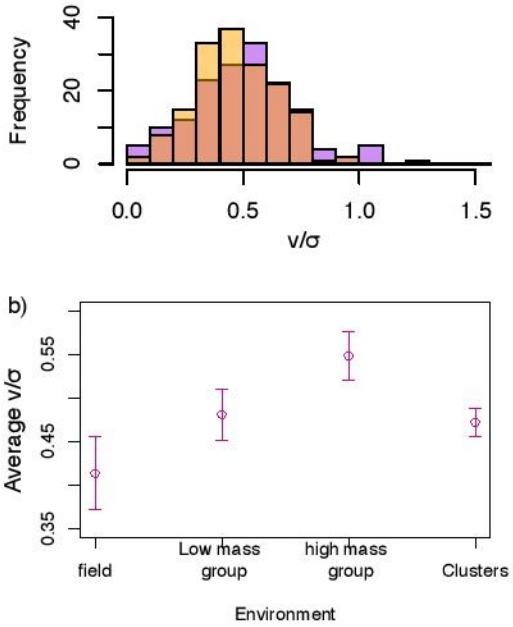

Figure 4. Distribution of v/σ values (a) for the GAMA (purple) and cluster (orange) regions, and the average stellar v/σ of S0s in the field, low mass groups (below $10^{13}M_{\odot}$, high mass groups (above $10^{13}M_{\odot}$) and the cluster regions (b).

Посмотрим глазами…

a) Pressure-supported S0s

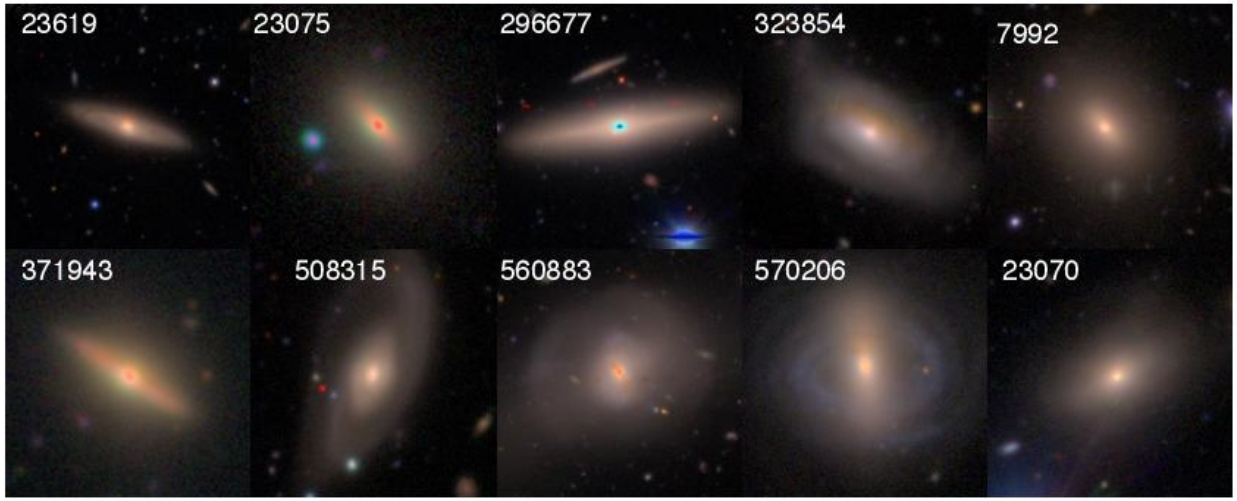

b) Rotationally-supported S0s

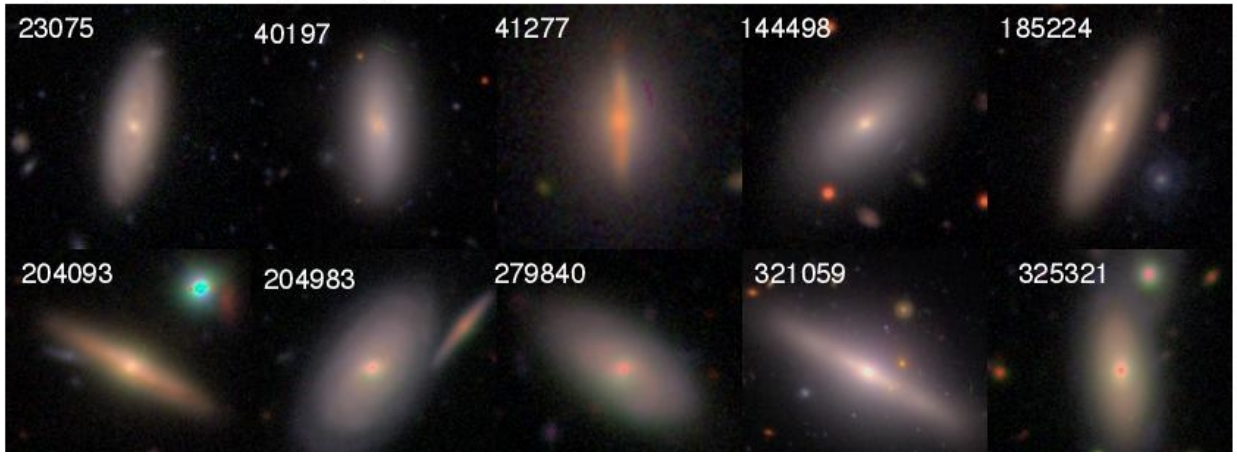

Сравним с эллиптическими…

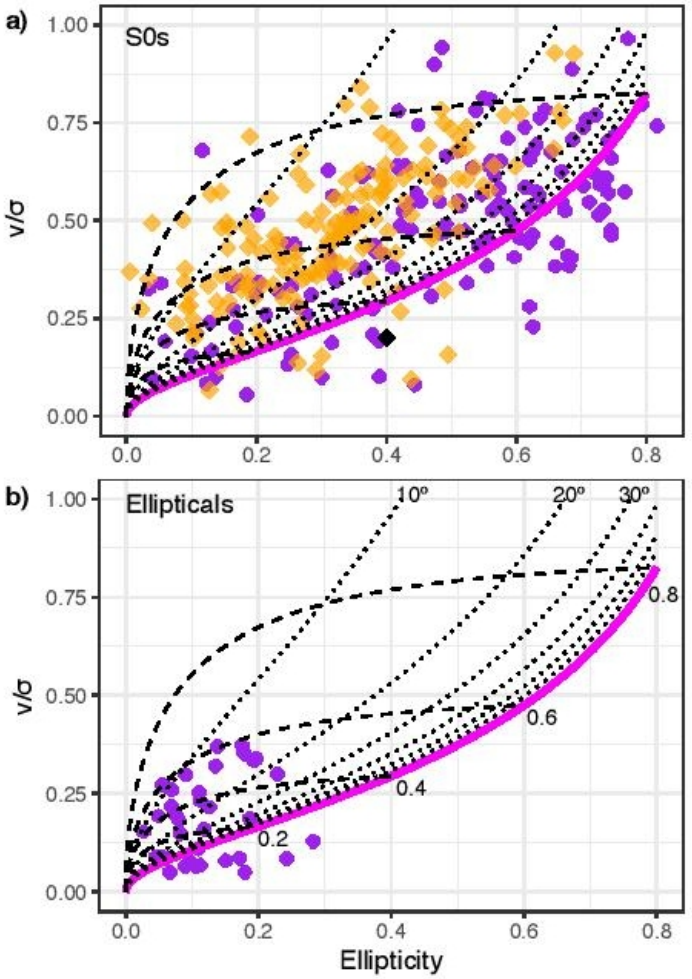

Figure 6. a) v/σ vs ellipticity for S0s in the GAMA (purp
circles) and cluster (orange diamonds) regions. The magenta li
shows the expected values for an edge-on axisymmetric gala

А вот про ионизованный газ:

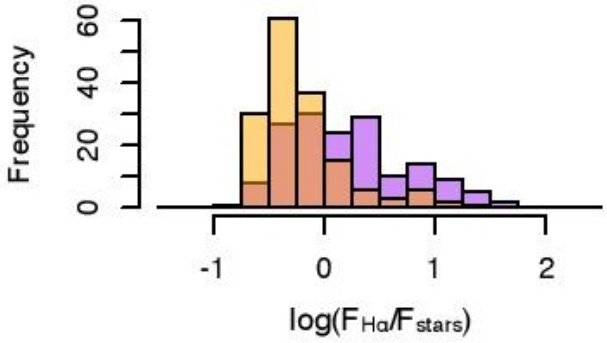

Figure 7. Distribution of the integrated $H\alpha$ flux to underlying continuum stellar flux ratio for S0s in the GAMA (purple) and cluster (orange) S0 regions. S0s in the clusters feature less gas emission than those in the rotationally-supported group.

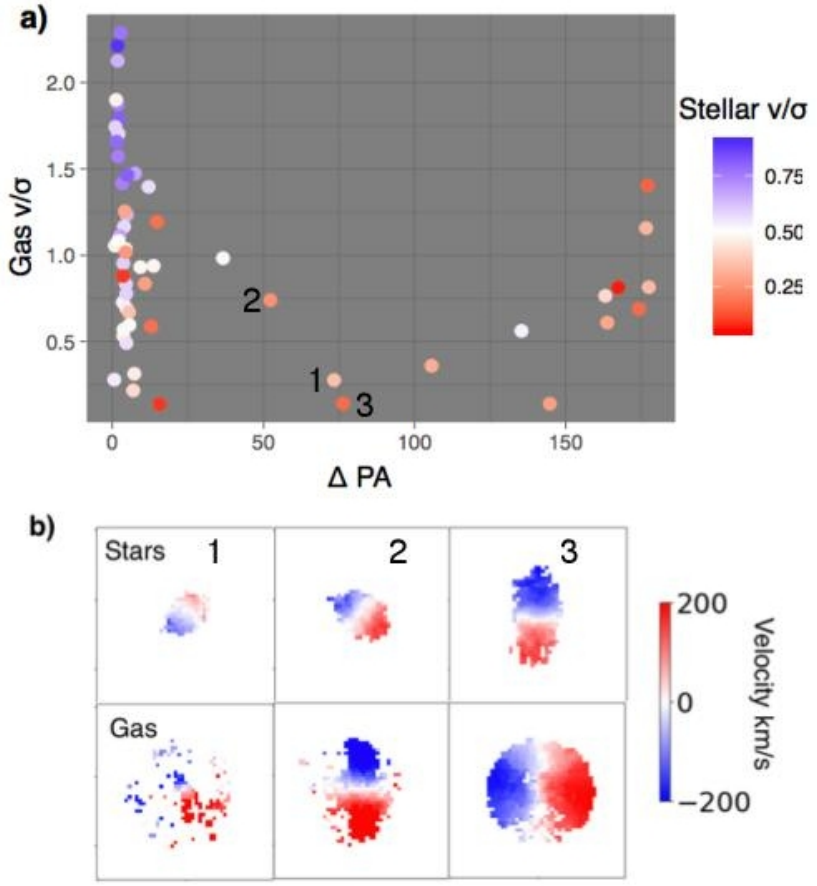

Примеры радиальных профилей

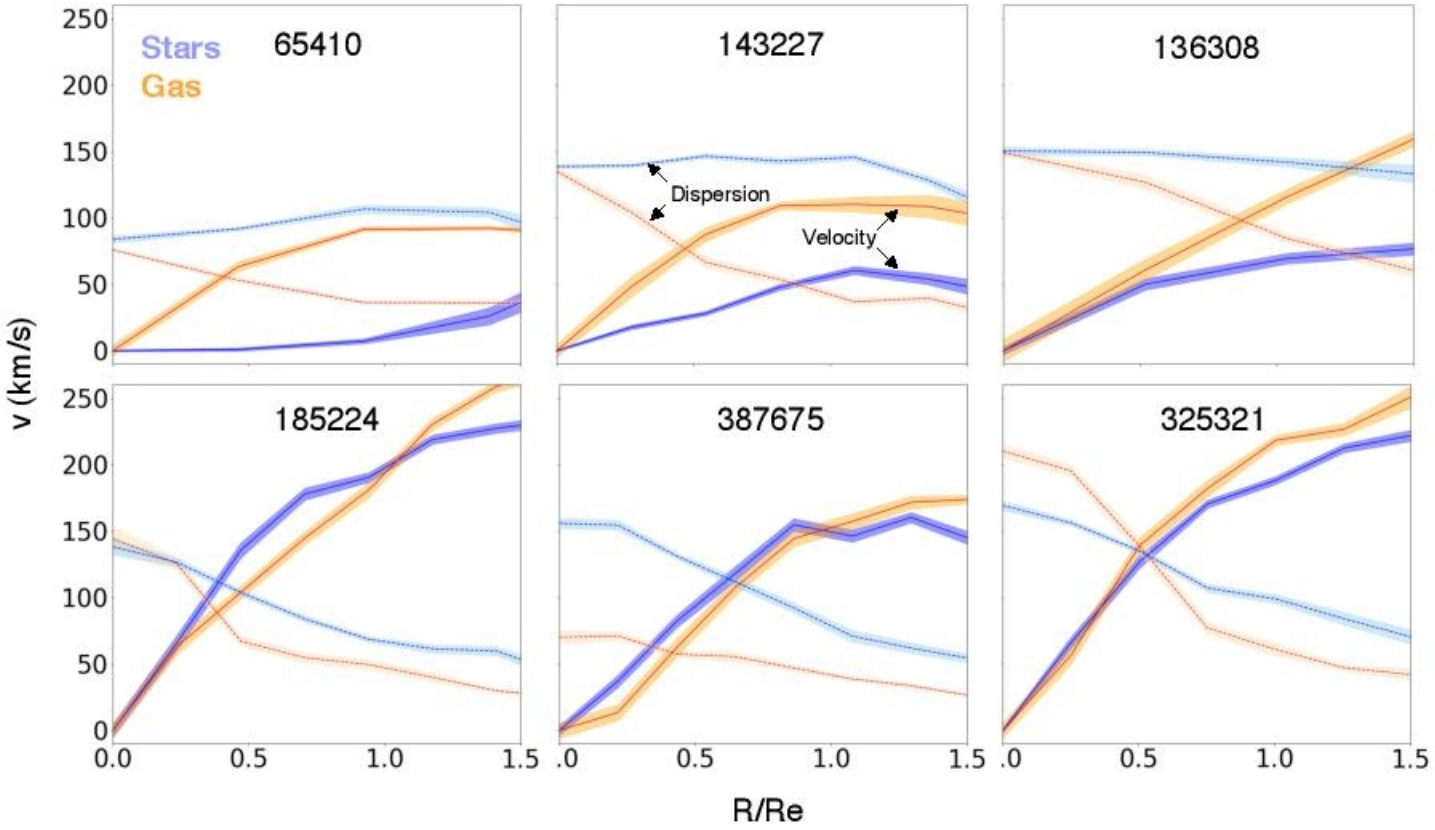

Figure 9. Stellar (blue) and gas (orange) kinematic profiles for S0s with v/σ below 0.5 (top row) and above 0.5 (bottom row). Solid lines are the velocities, dotted lines are the velocity dispersions. The pressure-dominated S0s feature gas rotation velocities significantly higher (at least two times faster at 1.5 Re) than the stellar components, while the rotation-dominated S0s feature gas velocities in line with their stellar components.

А вот наконец разобрались с «быстрыми ротаторами»…

and fast rotators. Slow rotators are defined to be those galaxies which fall within the region below $\lambda_{R_e} = 0.08 + e/4$ (Cappellari 2016). Recent work has suggested that slow and fast rotators may have different evolutionary pathways, with the slow rotators resulting from merger activity and the fast rotators following a more passive evolution (Penoyre, et al. 2017). However, the majority of early-type galaxies which fall within the slow-rotator class are ellipticals; for example in the work of Emsellem et al. (2007), while 10 out of 25 ellipticals are classed as slow rotators, only two out of 22 S0s are classed as slow rotators while the remaining were classed as fast rotators. Here we found the same behaviour for our S0 sample; only 12 out of 219 S0s lie within the slow-rotator region. This highlights that the spread in kinematics of S0s we find here lies in a different region of the ellipticity vs λ_{R_e} parameter space. Therefore we conclude that the spread in v/σ we observe is not caused by subpopulations corresponding to the slow and fast rotators, but is caused by a range of processes intrinsic within the S0 class.